Open access • Journal Article • DOI:10.1021/PR900451U

High precision quantitative proteomics using iTRAQ on an LTQ Orbitrap: a new mass spectrometric method combining the benefits of all. — Source link

Thomas Köcher, Peter Pichler, Michael Schutzbier, Christoph Stingl ...+5 more authors

Institutions: Research Institute of Molecular Pathology

Published on: 27 Aug 2009 - Journal of Proteome Research (American Chemical Society)

Topics: Top-down proteomics, Label-free quantification, Orbitrap and Quantitative proteomics

Related papers:

- Multiplexed Protein Quantitation in Saccharomyces cerevisiae Using Amine-reactive Isobaric Tagging Reagents
- Tandem Mass Tags: A Novel Quantification Strategy for Comparative Analysis of Complex Protein Mixtures by MS/MS
- Stable isotope labeling by amino acids in cell culture, SILAC, as a simple and accurate approach to expression proteomics.
- iTRAQ underestimation in simple and complex mixtures: "the good, the bad and the ugly".
- Robust and Sensitive iTRAQ Quantification on an LTQ Orbitrap Mass Spectrometer

research articles Journal of proteome research

High Precision Quantitative Proteomics Using iTRAQ on an LTQ Orbitrap: A New Mass Spectrometric Method Combining the Benefits of All

Thomas Köcher,*,† Peter Pichler,‡ Michael Schutzbier,† Christoph Stingl,† Axel Kaul,§ Nils Teucher,§ Gerd Hasenfuss,§ Josef M. Penninger,|| and Karl Mechtler†,||

Research Institute of Molecular Pathology (IMP), Vienna, Austria, Christian Doppler Laboratory for Proteome Analysis, University of Vienna, Vienna, Austria, University Medical Center Göttingen (UMG), Georg-August-Universität, Germany, and Institute of Molecular Biotechnology (IMBA), Vienna, Austria

Received May 20, 2009

The development of quantitative techniques in mass spectrometry has generated the ability to systematically monitor protein expression. Isobaric tags for relative and absolute quantification (iTRAQ) have become a widely used tool for the quantification of proteins. However, application of iTRAQ methodology using ion traps and hybrid mass spectrometers containing an ion trap such as the LTQ-Orbitrap was not possible until the development of pulsed Q dissociation (PQD) and higher energy C-trap dissociation (HCD). Both methods allow iTRAQ-based quantification on an LTQ-Orbitrap but are less suited for protein identification at a proteomic scale than the commonly used collisional induced dissociation (CID) fragmentation. We developed an analytical strategy combining the advantages of CID and HCD, allowing sensitive and accurate protein identification and quantitation at the same time. In a direct comparison, the novel method outperformed PQD and HCD regarding its limit of detection, the number of identified peptides and the analytical precision of quantitation. The new method was applied to study changes in protein expression in mouse hearts upon transverse aortic constriction, a model for cardiac stress.

Keywords: mass spectrometry • protein quantification • iTRAQ • mouse heart • cardiac stress model

Introduction

During the last two decades, mass spectrometry has become an indispensable tool in biological research. A plethora of novel methods, instruments and innovative strategies have been applied to numerous questions and have led to important insights in biology which would otherwise have been impossible to obtain.[1−4] While the main application of mass spectrometric methods in biology is still protein identification and the further characterization of proteins by analyzing their post-translational modifications,[5] there is growing interest in the relative and absolute quantification of proteins.[6,7] Partially, this trend originates from recent conceptual changes in biological research toward the description of biological systems with quantitative models.[8] Additionally, quantitative data can aid in discriminating contaminating proteins from true components of protein complexes[9] and can be used for characterizing their stoichiometry.[10−12] Furthermore, quantitative techniques have also been employed for quantifying post-translational modifications such as phosphorylation.[13] However, mass spectrometry is not quantitative *per se*. The signal strength corresponding to the individual peptide ions recorded in the mass spectrometer does not solely depend on the concentration of the peptides, but also on many other partly uncontrollable parameters such as signal suppression effects. In addition, sample preparation steps upstream of the mass spectrometric analysis also introduce irreproducible errors.

Several techniques have been developed to address these issues. The most elegant and precise methods are based on isotopic labeling for quantitation.[6,7] In these approaches, proteins are quantified by the ratios of the intensities of differentially labeled but chemically identical proteolytic peptides. When avoiding deuterium, changing the isotopic composition of molecules does not affect significantly their physical and chemical properties; therefore, the labeled samples can be readily analyzed by LC-MS/MS.[14] Aiming for relative quantification, samples corresponding to distinct biological conditions are differentially labeled. This can be done at various points during regular sample processing, starting from metabolic labeling[15] to differentially derivatizing proteins[16] or proteolytic peptides.[17] Regardless of the labeling procedure used, the ratios of the concentrations of the proteins present in the samples can be computed from the ratios of the signal intensities or the respective peak areas between the differentially labeled peptides corresponding to the same protein.

* To whom correspondence should be addressed. Thomas Köcher, Research Institute of Molecular Pathology (IMP), Vienna, Austria. Dr. Bohrgasse 7, A-1030 Vienna, Austria. Phone, 0043 1 79044 4283; fax, 0043 1 79044 110; e-mail, Thomas.Koecher@imp.ac.at.
† Research Institute of Molecular Pathology (IMP).
‡ University of Vienna.
§ Georg-August-Universität.
|| Institute of Molecular Biotechnology (IMBA).

Consequently, a significant complication relates to the ambiguity in assigning the identified peptides to individual proteins.[18,19]

In recent years, isobaric tags for relative and absolute quantification (iTRAQ)[17] have become increasingly popular for protein quantification, partly because the technique can be used for all protein sources not amenable to metabolic labeling such as human patient samples. The iTRAQ reagent contains a reporter group and an amino-reactive group, spaced by a mass balancing group, generating an identical mass shift for all tags. With the use of succinimide chemistry, the N-terminal amino group and the epsilon amino group of lysine residues of each peptide can be derivatized with the tag.[17] Relative quantitation of the differentially labeled peptides is achieved by their different fragmentation products. Each tag generates a unique reporter ion and the ratios between the signal intensities or peak areas of these reporter ions reflect the ratios of the peptides. The tags are commercially available in two forms, consisting of a set of four[17] or eight[20] different tags. Generation of reporter ions by fragmentation is usually achieved by collisional induced dissociation (CID)[17] but was also shown for electron transfer dissociation (ETD).[21,22] Commonly, the 4-plex reagent is used, generating the singly charged reporter ions with m/z values of 114.111, 115.108, 116.112, and 117.115 after CID fragmentation.[17]

A broad range of instruments is capable of analyzing iTRAQ labeled peptides such as quadrupole-time-of-flight (Q-ToF)[23] or tandem time-of-flight (ToF/ToF)[24] mass spectrometers. However, iTRAQ-based quantitation under standard CID conditions is not feasible on ion traps because of their low mass cutoff limitation, prohibiting the analysis of product ions with m/z values less than 25−30% of the precursor ion. More importantly, this limitation also applies to hybrid instruments containing an ion trap for fragmentation such as the LTQ-FT (linear ion trap-Fourier transform ion cyclotron resonance hybrid mass spectrometer) and the LTQ-Orbitrap. In the last 2 years, the LTQ-Orbitrap[25−27] has become the instrumentation of choice for many proteomic laboratories. Without compromising the overall throughput of measurements, this instrument combines the fast duty cycle of linear ion traps for MS/MS along with the high resolution and high mass accuracy capabilities of the Orbitrap.

Recently, two methods have been introduced, called pulsed Q dissociation (PQD)[28] and higher energy C-trap dissociation (HCD)[29] which both allow analysis of the low m/z region of iTRAQ reporter ions. However, both methods are less suited for protein identification than regular CID fragmentation in the ion trap.

Here, we describe a new approach, which by combining the benefits of HCD performed in an octopole collision cell and CID in the linear ion trap greatly enhances the analytical capabilities of the LTQ-Orbitrap for analyzing iTRAQ labeled peptides. Comparing HCD, PQD and the new method, which we call CID-HCD, we found CID-HCD to be superior to both PQD and HCD in terms of its sensitivity and ability to identify proteins in complex protein mixtures. We further demonstrated the practical utility of the novel approach by analyzing changes in protein expression in mouse hearts upon transverse aortic constriction using two-dimensional LC-MS/MS.

Material and Methods

Sample Preparation. C57bl6 wild-type animals from a rederived mouse strain underwent TAC (transverse aortic constriction) as a model of biomechanical stress, or sham surgery at 8 weeks of age. TAC was performed as minimally invasive MTAB (minimally invasive transverse aortic banding) as described previously.[30] Cardiectomy was performed 1 day after echocardiography. Time from cardiectomy to freezing the samples in liquid nitrogen was less than 30 s. Left ventricles were isolated, ground in liquid nitrogen and shipped on dry ice. One milliliter of ice-cold lysis buffer (50 mM HEPES-KOH, pH 7.5, 5 mM EDTA, 150 mM KCl, 10% (v/v) glycerol, 1% (v/v) Triton X-100, 20 mM betaglycerophosphate, 10 mM NaF, 10 mM Na-pyrophosphate, 1× Protease Inhibitor Mix (PIM, 1000×: 10 mg/mL each of leupeptin, pepstatin and chymostatin, in DMSO), 0.1 mM PMSF, 1 mM Na_3VO_4, 1 mM DTT) was added to 15 mg of sample, followed by sonication and Potter homogenization on ice and centrifugation at 13 000 rpm for 10 min at 4 °C. The supernatant was transferred to a fresh tube, and protein concentration was determined by BCA assay before and after acetone precipitation for protein purification. One left ventricle from a TAC mouse and one left ventricle from a sham-operated mouse were processed in an identical manner.

iTRAQ Labeling and Protein Digestion. Proteins were tryptically digested and the resultant peptide mixture was labeled using chemicals from the iTRAQ reagent kit (Applied Biosystems; Foster City, CA) essentially as previously described.[17] Briefly, proteins were dissolved in 0.5 M triethylammonium bicarbonate (TEAB), adjusted to pH 8. Disulfide bonds were reduced in 5 mM Tris-(2-carboxyethy) phosphine (TCEP) for 1 h at 60 °C, followed by blocking cysteine residues in 10 mM methylmethanethiosulfonate (MMTS) for 30 min at room temperature, before digestion with mass spectrometry-grade modified trypsin (Promega, Madison, WI). For labeling, each iTRAQ reagent was dissolved in 70 μL of ethanol and added to the respective peptide mixture. Prior to LC-MS/MS, reactions were stopped with 0.1% TFA and the four samples were mixed. Ethanol was removed by drying down the solvent to 2−4 μL in a vacuum centrifuge. The peptide mixture was again dissolved in 0.1% TFA.

HPLC and Mass Spectrometry. For strong cation exchange (SCX) chromatography, 220 μg of the labeled peptide mixtures was fractionated on a Polysulfethyl A Column (20 cm × 2.1 mm × 5 μm, 200 Å PolyLC, Inc.). First, the mixed samples were lyophilized, dissolved and loaded in buffer A (5 mM sodium phosphate, pH 2.7, 15% acetonitrile (ACN)). Peptides were eluted by a pH and salt gradient using buffer B (5 mM sodium phosphate, pH 2.7, 1 M NaCl, 15% ACN) and buffer C (10 mM sodium phosphate, pH 6.0, 20% ACN) The gradient was as follows: 0−15 min, 100% A; 15−45 min, 15% B, 15% C; 45−60 min, 25% B, 25% C; 60−70 min, 30% B, 30% C; 71−75 min, 50% B, 50% C; 75−90 min, 60% B, 40% C; 91−120 min, 100% A. A total of 96 fractions were collected at a flow rate of 150 μL/min. The volume of the fractions was evaporated to approximately 100 μL in a speed-vacuum centrifuge diluted to 200 μL with 0.1% TFA, and 100 μL was analyzed by LC-MS/MS.

Nano-HPLC-MS/MS analysis was performed on a Dual Gradient Ultimate 3000 HPLC system (Dionex). Peptide separation was carried out on a C18 column (Acclaim PepMap C18, 15 cm × 75 μm × 3 μm, 100 Å, Dionex) using the following solvent system: A, 5% ACN, 0.1% formic acid; B, 30% ACN, 0.08% formic acid; C, 80% ACN, 0.08% formic acid, 10% trifluoroethanol. For the sensitivity experiment with the peptide mixture generated from BSA, we used a short gradient from 100% A to 100% B (21 min), followed by a short gradient to 80% B and 20% C (5 min). For the other experiments, we used

a gradient from 100% A to 30% B (95 min), from 30% B to 100% B (145 min) followed by a 30 min gradient from 0% B and 50% C to 90% C. The HPLC was directly coupled to a nanoelectrospray ionization source (Proxeon, Odense, Denmark).

The LTQ-Orbitrap XL mass spectrometer (Thermo-Fisher Scientific) was operated in positive ionization mode. The MS survey scan for all experiments was performed in the FT cell recording a window between 300 and 1500 m/z. The resolution was set to 60 000 and the automatic gain control (AGC) was set to 500 000 ions. The m/z values triggering MS/MS were put on an exclusion list for 240 s. The minimum MS signal for triggering MS/MS was set to 500. In all cases, one microscan was recorded. The lock mass option was enabled for both MS and MS/MS mode and the polydimethylcyclosiloxane ions (protonated $(Si(CH_3)_2O))_6$; m/z 445.120025) were used for internal recalibration of the mass spectra.[31]

For HCD, the applied acquisition method consisted of a survey scan to detect the peptide ions followed by a maximum of four MS/MS experiments of the four most intense signals exceeding a minimum signal of 500 in survey scans. For MS/MS, we used a resolution of 7500, an isolation window of 4 m/z and a target value of 300 000 ions, with maximum accumulation times of 1 s. Fragmentation was performed with normalized collision energy of 40% and an activation time of 40 ms.

For PQD, we again used four dependent MS/MS experiments, with normalized collision energy of 40%, a Q value of 0.6, and an activation time of 0.1 ms. Fragment ions were recorded in the linear ion trap using a target value of 10 000 ions.

The CID-HCD acquisition method consisted of four sets of dependent MS/MS scans, with a CID and a HCD tandem mass spectrometry experiment triggered from the same precursor ion. CID was done with a target value of 10 000 in the linear ion trap, collision energy of 35%, Q value of 0.25 and an activation time of 30 ms. HCD-generated ions were detected in the Orbitrap using a target value of 300 000, collision energy of 55% and an activation time of 40 ms.

Data Interpretation. For CID-HCD data sets, data processing was performed using a Perl script (QuantMerge). In short, intensities from the 4 iTRAQ reporter ions, m/z 114.112, 115.1083, 116.116, and 117.1150, were extracted from the Mascot-generated mgf-file of each HCD spectrum with a mass tolerance of 10 mDa. The intensities of the reporter ions were normalized to 1 and were pasted into the corresponding CID spectrum, deleting at the same time the respective m/z region of the original CID spectrum. The number of paired and merged spectra and the number of unassigned spectra are reported. The script will be available on our Web page: (http://www.imp.ac.at/research/protein-chemistry/labhomepage/).

Fragment ion data were interpreted using Mascot. Data from the BSA experiments were searched against Swiss-Prot database. Data generated from the mouse samples were searched against the mouse International Protein Index (IPI) database. In all cases, a peptide mass tolerance of 5 ppm was used and fragment ion masses were searched with a 0.5 Da mass window. One missed cleavage site for trypsin was allowed. Methylthiocysteine and iTRAQ reagent labeling at the N-terminus and lysine residues were set as fixed modifications. Variable modifications included oxidation of methionine, and phosphorylation of serine, threonine, and tyrosine. Identified proteins were grouped and further analyzed with Protein Center (v2.5.0. Proxeon Biosystems, Odense, Denmark). Protein grouping was based on 98% homology. Quantitation of iTRAQ labeled peptides was performed with Mascot using the isotopic corrections supplied by the manufacturer (Applied Biosystems; Foster City, CA).

Results

Both PQD and HCD enable iTRAQ-based quantification on an LTQ-Orbitrap mass spectrometer. However, PQD suffers from very poor fragmentation efficiency and low product ion counts when compared to CID,[32,33] and is naturally less suited for precise quantitation. HCD fragmentation, on the other hand, offers high fragmentation efficiency, especially after introduction of an additional octopole dedicated for fragmentation. The fragment ions generated have to be detected in the Orbitrap part of the instrument, whereas PQD allows detection of fragment ions in the linear ion trap. Consequently, HCD is limited by the lower duty cycle of the Orbitrap, however, with the advantage of its high mass accuracy.[29] Recently, PQD and HCD have been compared, and it was reported that PQD is better suited for identification and quantitation than HCD with respect to the achievable sensitivity.[33] However, several issues should be considered before coming to a final conclusion regarding the best strategy for iTRAQ quantification with an LTQ-Orbitrap. First, HCD performed in the Orbitrap allows mass accuracies much better than 5 ppm,[31] with obvious advantages not only for protein identification, but also for quantitation.[34,35] It should be noted, however, that Mascot treats all m/z values within the allowed mass window uniformly and does not score properly for high mass accuracy. Second, although HCD and PQD are both capable of generating b- and y-ions ions needed for peptide identification, the overall sensitivity of these two methods is still much lower than CID performed and detected in the linear ion trap of the LTQ-Orbitrap.

Hybridization of CID and HCD. We reasoned that, by combining the strengths of CID and HCD, the overall performance of the LTQ-Orbitrap regarding iTRAQ-based protein quantification can be increased. To this end, we designed an acquisition scheme consisting of alternating CID and HCD tandem mass spectrometry experiments. For each precursor ion, first a CID spectrum is generated and recorded in the linear ion trap, followed by the acquisition of a HCD spectrum from the same peptide ion. The CID spectrum will be used for identification of the peptide, while the HCD spectrum will be used solely for the reporter ion based quantification (Figure 1). A similar approach was published combining PQD and CID.[36] While the latter strategy also exploits CID for efficient peptide identification, it will still inevitably suffer from the intrinsic weaker quantification capabilities associated with the low ion counts achievable with PQD. In addition, iTRAQ reporter ions are detected with high mass accuracy in the CID-HCD hybrid method, avoiding quantification of interfering signals with close m/z values. Straightforward interpretation of the data sets generated is possible with software capable of searching and interpreting combined CID and HCD data sets such as Proteome Discoverer (Thermo Fisher Scientific). The other option is to merge the data of the iTRAQ reporter ions of each acquired HCD spectrum with the CID spectrum acquired from the same precursor. We generated a software tool for merging and processing the CID-HCD data set (Figure 1). First, the iTRAQ reporter ions are extracted from each HCD spectrum and their intensity values normalized to one. Second, if present, the tool removes the reporter ion specific m/z region

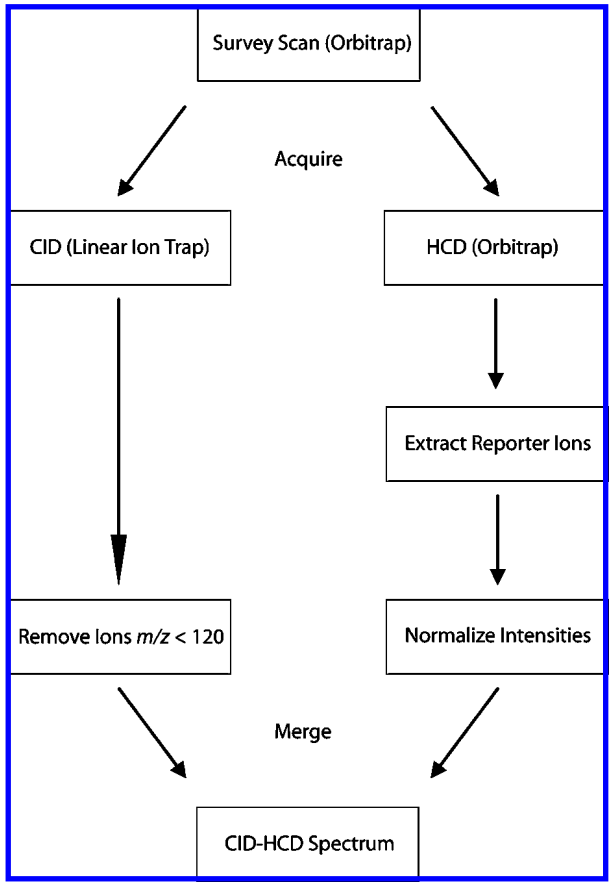

Figure 1. Overview of the analytical strategy of CID-HCD and the data processing. For each precursor ion detected in the Orbitrap, a CID spectrum and a HCD spectrum are generated. For HCD (right side), iTRAQ reporter ions are extracted with a defined mass accuracy and these values are normalized to 1. For CID (left side), values below *m/z* 120 are removed from the data. The extracted values of the reporter ions are merged with the CID data to generate a mixed CID-HCD spectrum for each precursor ion.

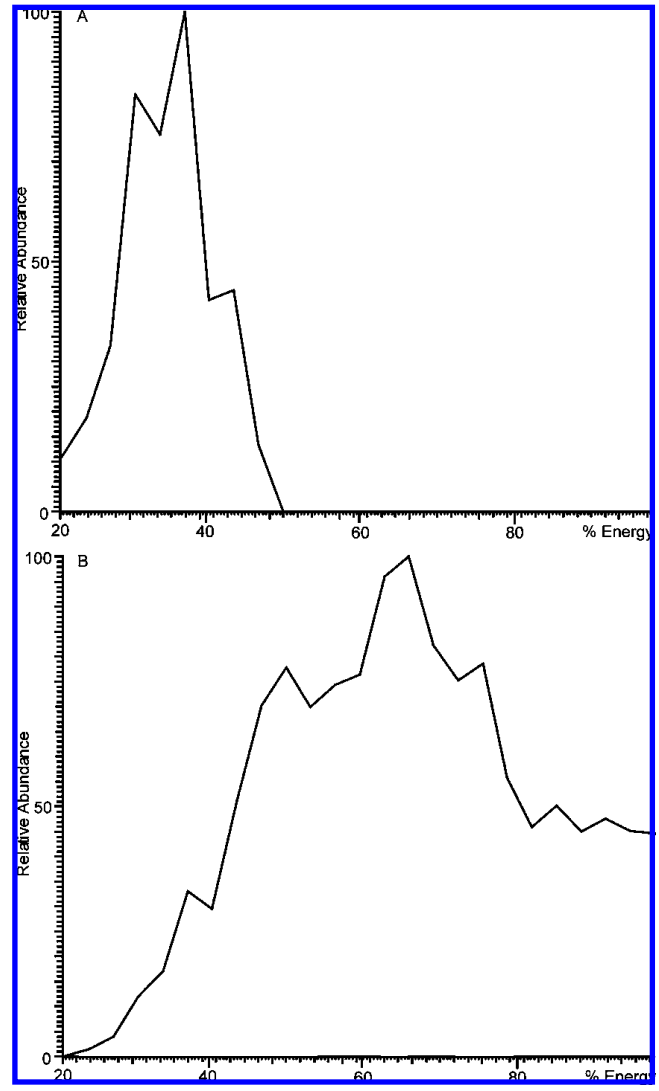

Figure 2. Optimization of collisional energy for CID-HCD. (A) The relative abundance of y_4 of the peptide LCVLHEK upon variation of the applied CE in HCD is shown. (B) The abundance of iTRAQ reporter ions generated upon ramping of CE for the same peptide.

from the corresponding CID spectra. Finally, the extracted values of the four iTRAQ channels are merged with the respective CID data. It should be noted that the intensities of iTRAQ reporter ions should be normalized to low ion counts, because otherwise Mascot peptide scores can be significantly reduced. This effect is caused by the higher ion counts of the reporter ions in HCD, resulting from different target values and ion injection times. As a consequence, the most abundant fragment ions are not sequence-specific ions, and the resulting peptide score is decreased.

Optimization of HCD Energy Settings for the CID-HCD Method. The CID-HCD method also has the immediate advantage that HCD fragmentation can be optimized for generation of iTRAQ reporter ions, with an optimum of normalized collisional energy (CE)[37] not necessarily ideal for peptide sequencing. To evaluate the relationship between applied collision energy and generation of b-, y-, and reporter ions, iTRAQ labeled tryptic peptides from BSA were analyzed. With the use of direct infusion nanoelectrospray, the fragmentation energy for HCD was ramped from 20% up to 100% normalized CE. In these experiments, it became evident that the relative intensities of b- and y-ions peak when the applied normalized collision energy is between 30% and 40% (Figure 2A). In contrast, we did not observe a clear maximum for the iTRAQ reporter ions but rather a plateau starting from 40% to 60% normalized CE (Figure 2B). Generally, maximal efficiency of reporter ion generation requires higher energy settings than for peptide sequencing. In addition, selection of optimal CE settings for b- and y-ion formation seems to be more critical for HCD than for CID in an ion trap.

Limit of Detection and Quantification for HCD, PQD, and CID-HCD. After defining optimal mass spectrometric conditions for PQD, HCD, and CID-HCD, the three approaches were compared regarding their limits of detection and quantification. We investigated the minimum amount of tryptically digested BSA needed for protein identification requiring at least two matching peptides with a Mascot peptide score greater than 25 and at least one of them containing all four iTRAQ reporter ions. Each method was challenged with a dilution series of iTRAQ labeled peptide mixtures using LC-MS/MS. Using a 100:100:200:200 amol peptide mixture, we could identify and quantify BSA with both PQD and CID-HCD, although with substantial differences regarding the number of

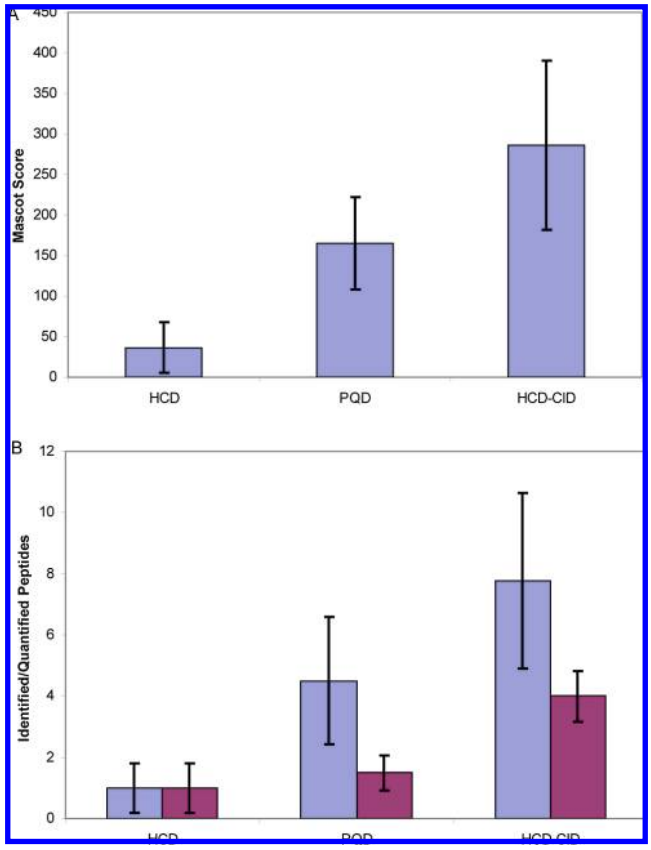

Figure 3. (A) Mascot scores of the four technical repeats of the three methods with iTRAQ labeled BSA are shown. With PQD, we obtained a mean Mascot protein score of 164.75, whereas with CID-HCD, the value was 286.5. (B) The numbers of identified and quantified peptides for the three methods are shown. Numbers (average number and standard deviation) of identified (blue) and quantified (red) peptides are shown for the three methods (four technical repeats).

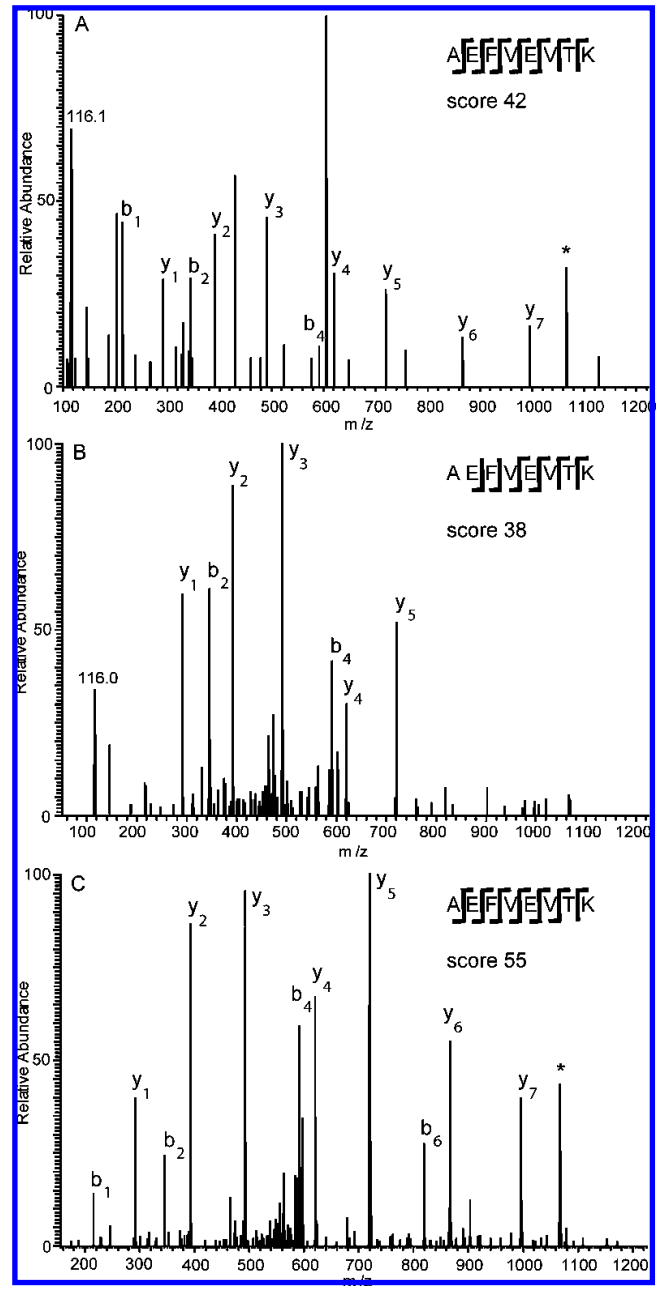

Figure 4. The impact of the three methods on the achieved data quality is illustrated with the iTRAQ-labeled peptide AEFVEVTK. Observed b- and y-ions and the iTRAQ reporter ion are annotated. Peaks marked with an asterisk represent ions after loss of the complete iTRAQ tag. (A) With HCD, 12 of the 14 theoretically observable b- and y-ions ions were detected leading to a Mascot ions score of 42. (B) Fragmentation by PQD of the same peptide leads to a better signal-to-noise ratio, but only 8 b- and y- ions were identified and a Mascot ions score of 38 was achieved. (C) In the CID spectrum of the same peptide, 13 out of 14 cleavage products were found. With CID-HCD, a peptide score of 55 was achieved which was based on the higher number of fragment ions and the significantly higher signal-to-noise ratio.

detected and identified peptides and their peptide scores as well as the total cumulative Mascot protein score (Figure 3). In our analytical setting, 100 amol was found to be the limit of quantification for both PQD and CID-HCD because we failed to quantify 50 amol of the same peptide mixture.

Using HCD with a CE of 40% and an activation time of 40 ms, we failed to robustly identify 100 amol BSA. Repeating the experiment four times, we identified BSA in only one case with two peptides, yielding a total Mascot protein score of 75 (Figure 3A). In the remaining three experiments, we could not identify BSA with at least two matching peptides, our above-mentioned requirement. On average, we identified and quantified BSA in the four technical replicates with only one peptide.

For PQD, we used a CE of 40%, a *Q* value of 0.6 and an activation time of 0.1 ms. It should be noted that the optimal CE range for specific *Q* values and activation times does not seem to be a stable setting for all LTQ instruments. Different values have been published[28,32,33] and we and others[28] noticed that even on the same instrument optimal settings might fluctuate over time. However, as already mentioned, fragmentation efficiency is rather low in PQD, leading to low total ion currents in these experiments. After optimization, the relative intensities of the iTRAQ reporter ions are in the same range as the sequence-specific b- and y-ions, allowing simultaneous quantitation and identification. For each survey scan in the Orbitrap, four PQD spectra were acquired in the linear ion trap. As reported previously, PQD performs considerably better than HCD when analyzing minute amounts of proteins.[33] With PQD, we identified BSA in all four technical replicates. Requiring a peptide score of 25, the average protein Mascot score was 165 with an average number of 4.5 identified peptides (Figure 3).

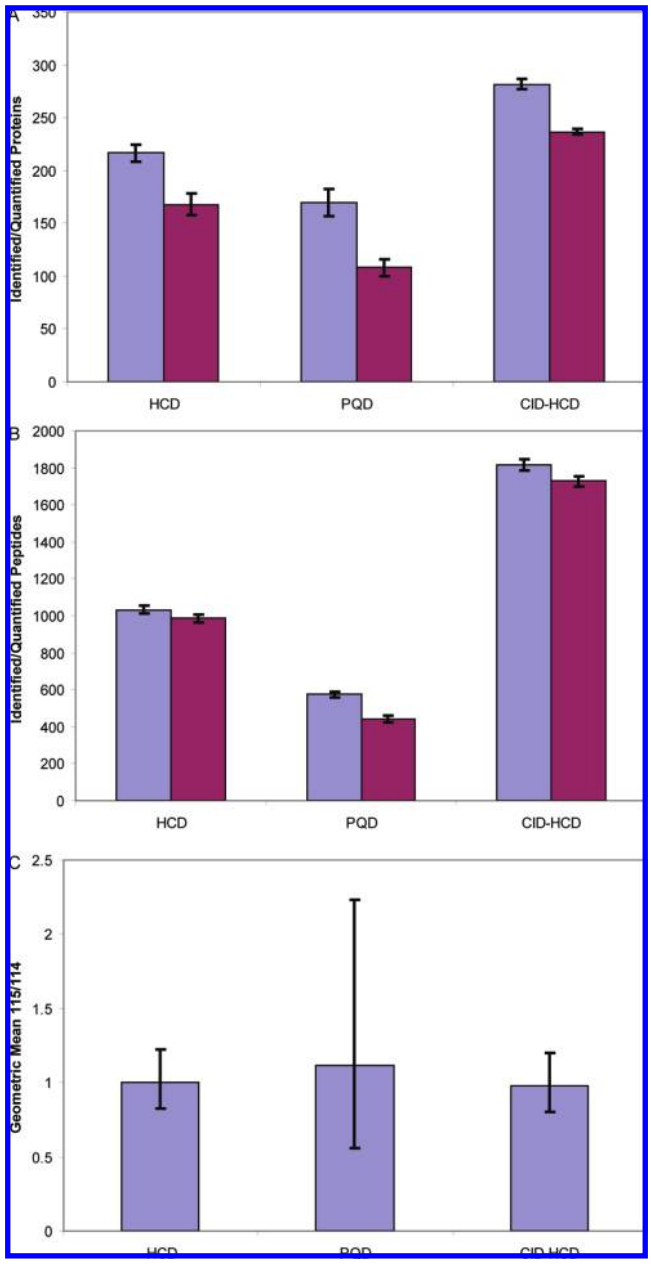

Figure 5. The three methods are compared in LC-MS/MS experiments with regard to the number of identified (blue) and quantified proteins (red) (A), the number of identified (blue) and quantified (red) peptides with a Mascot ion score better than 25 (B) and the mean value of the iTRAQ channels 115/114 for all peptides and the geometric standard deviation of these ratios (C).

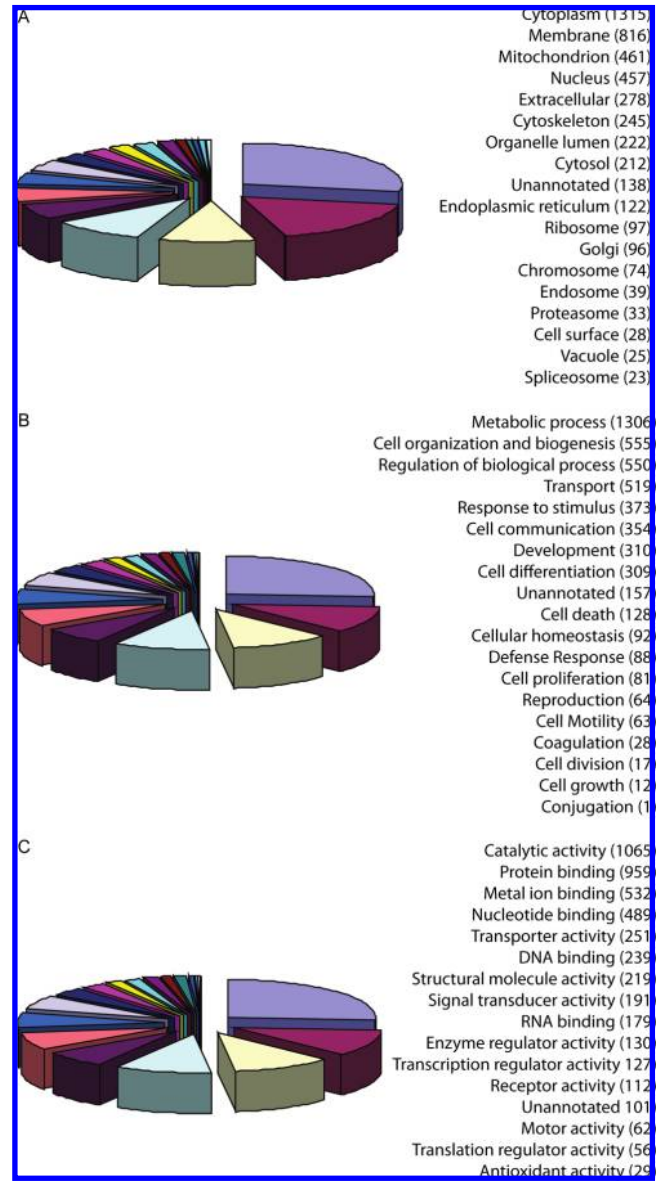

Figure 6. GO analysis of the data set from the two-dimensional LC-MS/MS experiment. The graphs show the numbers of proteins assigned to (A) specific molecular functions, (B) cellular components and (C) biological processes.

However, many of the identified peptides were lacking one ore more iTRAQ reporter ions; therefore, the average number of quantified peptides was only 1.5. The geometrical means of all peptide ratios averaged over the four measurements were 0.9 for 115/114, 2.2 for 116/114, 2.6 for 117/114, and 1.2 for 117/116, with standard deviations in the range of 1.3.

Finally, we analyzed the peptide mixture with our novel analytical strategy. After the survey recorded in the Orbitrap, we acquired four sets of a CID spectrum measured in the linear ion trap, followed by a HCD spectrum from the same precursor in the Orbitrap. HCD was performed with the relatively high normalized CE of 55% and an activation time of 40 ms. As expected, in these experiments, the average number of matching peptides increased substantially to 7.8, resulting in a cumulative Mascot protein score of 287 (Figure 3). The average number of quantified peptides was 4, and the geometric mean of the peptide ratios was 115/114 = 0.9, 116/114 = 2.5, 117/114 = 2.5 and 117/116 = 1, again with standard deviations of approximately 1.2.

Summarizing these results, both PQD and the CID-HCD method allow the relative quantitation of 100 amol iTRAQ labeled BSA peptides in a 100:100:200:200 amol peptide mixture. With very similar time demands for all three methods, PQD clearly outperforms the HCD method in all aspects, but using the CID-HCD method, we obtained significantly better figures of merit than with PQD.

These results were also evident by visual inspection and interpretation of the tandem mass spectra obtained with the three methods. We observed a higher number of sequence

specific cleavage products and a higher signal-to-noise ratio with CID-HCD than with the other methods (Figure 4).

Performance of HCD, PQD, and CID-HCD in the Analysis of Complex Protein Mixtures. We evaluated the performance of the three methods in the analysis of a complex protein mixture regarding the number of proteins and peptides identified and quantified. Application of the CID-HCD method results in a slightly prolonged duty cycle which might decrease the number of identified proteins when compared to the two other methods. For this purpose, we analyzed a complex protein mixture generated from mouse hearts after either transaortic constriction (TAC) or sham surgery. We again performed a double labeling procedure, splitting each sample into two identical aliquots before performing the iTRAQ labeling and analyzing technical triplicates using an LC gradient of 4.5 h of effective separation time with each method. For identification, a Mascot peptide score of at least 25 and a significance threshold of at least 0.01 was required for protein identification. For quantification, we demanded quantitative data from at least two tandem mass spectra.

Data interpretation of the three triplicates clearly showed that CID-HCD outclassed the other two methods regarding the number of proteins and peptides identified and quantified (Figure 5A,B). On the basis of 1033 peptides, 985 with all four reporter ions present, the HCD data set led to the identification and quantification of an average number of 217 and 168 protein

Table 1. Proteins Identified in the 2D-LC-MS/MS Experiment, Up-Regulated at Least 1.5-fold Are Listed with Their Corresponding iTRAQ Ratios

accession number	description	gene symbol	115/114	116/114	117/114
IPI00453998	ankyrin repeat domain 1 (cardiac muscle)	Ankrd1	1.131	4.221	4.644
IPI00120870	periostin; osteoblast specific factor	Postn	0.899	3.311	3.06
IPI00309997	four and a half LIM domains 1 isoform 3	Fhl1	0.937	3.174	3.011
IPI00128791	heat shock protein; alpha-crystallin-related; B6	Hspb6	0.938	2.757	2.783
IPI00109910	Ighg protein	Ighg	0.623	2.693	2.663
IPI00323600	coronin; actin binding protein 1A	Coro1a	0.884	2.734	2.597
IPI00406213	similar to Chain L; Structural Basis Of Antigen Mimicry In A Clinically Relevant Melanoma Antigen System isoform 1	#N/A	0.85	2.347	2.375
IPI00121013	phosphoprotein enriched in astrocytes 15 isoform 2	Pea15a	0.948	2.192	2.293
IPI00396671	ATP-binding cassette; subfamily F (GCN20); member 1	Abcf1	1.029	2.201	2.275
IPI00469392	reticulon 4 isoform A	Rtn4	1.012	2.299	2.264
IPI00170232	supervillin isoform 1	Svil	1.268	2.098	2.255
IPI00114733	Serpin H1	Serpinh1	1.003	2.234	2.218
IPI00227871	very large inducible GTPase 1	Gvin1	1.011	2.306	2.182
IPI00118736	protein phosphatase 1B isoform 1	Ppm1b	1.107	1.885	2.181
IPI00117556	Heat shock protein beta-7	Hspb7	0.945	2.203	2.174
IPI00224784	prothymosin alpha	Ptma	0.862	1.959	2.174
IPI00284242	Isoform 1 of Protein enabled homologue	Enah	1.01	1.988	2.169
IPI00403810	tubulin; alpha 1C	Tuba1c	1.01	2.196	2.153
IPI00110753	tubulin; alpha 1	Tuba1a	1.01	2.196	2.153
IPI00129685	Translationally controlled tumor protein	Tpt1	1.618	1.98	2.118
IPI00177047	Sorbs2 protein	Sorbs2	1.016	2.149	2.116
IPI00230395	annexin A1	Anxa1	1.017	2.05	2.103
IPI00118892	lymphocyte cytosolic protein 1	Lcp1	0.986	2.112	2.096
IPI00119111	calponin 3; acidic	Cnn3	1.041	2.228	2.067
IPI00119305	ErbB3-binding protein 1	Pa2g4	1.241	2.13	2.05
IPI00128522	heat shock protein 1	Hspb1	0.908	2.028	2.049
IPI00114162	fatty acid binding protein 5; epidermal	Fabp5	0.976	2.092	2.047
IPI00135186	calumenin isoform 1	Calu	0.927	2.136	2.036
IPI00406447	Collapsin response mediator protein 4A	Dpysl3	0.927	2.375	2.035
IPI00134206	matrix-remodelling associated 7	Mxra7	1.306	2.18	2.031
IPI00461969	D123 gene product	Cdc123	1.247	2.09	2.024
IPI00129959	SEC8	Exoc4	0.831	2.151	2.01
IPI00223047	cytoskeleton-associated protein 4	Ckap4	0.953	2.187	2.001
IPI00138274	crystallin; alpha B	Cryab	0.954	2.031	1.998
IPI00117350	tubulin; alpha 4	Tuba4a	0.976	2.053	1.997
IPI00117352	tubulin; beta 5	Tubb5	0.931	2.024	1.979
IPI00128703	paxillin isoform alpha	Pxn	0.947	1.801	1.973
IPI00137331	Adenylyl cyclase-associated protein 1	Cap1	0.87	2.061	1.969
IPI00229534	myristoylated alanine rich protein kinase C substrate	Marcks	1.07	2.03	1.968
IPI00329872	collagen; type I; alpha 1	Col1a1	1.087	2.063	1.956
IPI00125778	transgelin 2	Tagln2	0.919	2	1.95
IPI00311175	tubulin; alpha 8	Tuba8	0.935	1.983	1.944
IPI00664670	Isoform 1 of Filamin-C	Flnc	1.023	2.009	1.917
IPI00221494	LIM domain containing preferred translocation partner in lipoma isoform 1	Lpp	0.907	2.069	1.913
IPI00112223	EF-hand domain-containing protein D2	Efhd2	0.872	2.021	1.89
IPI00314106	cat eye syndrome chromosome region; candidate 5 homologue precursor	Cecr5	1.115	2.098	1.831
IPI00399953	WNK lysine deficient protein kinase 1	Wnk1	1.135	1.979	1.829

Table 2. Proteins Identified in the 2D-LC-MS/MS Experiment Down-Regulated at Least by a Factor of 0.67

accession number	description	gene symbol	115/114	116/114	117/114
IPI00467841	unnamed protein product	Calm1	0.888	0.874	0.881
IPI00134484	translocase of inner mitochondrial membrane 9 homologue	Timm13	0.801	0.872	0.779
IPI00133403	NADH dehydrogenase (ubiquinone) 1 beta subcomplex 3	Ndufb3	0.817	0.871	0.899
IPI00648053	mCG2330; isoform CRA_a	Tomm5	0.869	0.86	0.892
IPI00458879	leucine-rich repeat kinase 1	Lrrk1	0.88	0.857	0.846
IPI00853920	PREDICTED: similar to thioredoxin reductase 2	#N/A	1.031	0.844	1.168
IPI00228106	hypothetical protein LOC216792	#N/A	0.834	0.844	0.906
IPI00153579	mono(ADP-ribosyl)transferase; ART3	Art3	0.925	0.839	0.822
IPI00122499	Transmembrane protein 143	Tmem143	0.937	0.817	0.85
IPI00129516	ubiquinol-cytochrome c reductase hinge protein	Uqcrh	0.905	0.79	0.791
IPI00221580	hypothetical protein LOC67892	#N/A	0.831	0.757	0.648
IPI00225390	cytochrome c oxidase subunit VIb polypeptide 1	Cox6b1	0.92	0.736	0.733
IPI00132169	translocase of inner mitochondrial membrane 8 homologue b	Timm8b	0.818	0.735	0.733
IPI00125460	ATP synthase; H+ transporting; mitochondrial F0 complex; subunit F	Atp5j	1.056	0.644	0.655
IPI00474783	acetyl-Coenzyme A carboxylase alpha	Acaca	0.814	0.559	0.529

groups, respectively. With PQD, we identified 170 and quantified an average number of 108 protein groups.. Counting again only peptides matching to identified proteins, the average number of identified peptides was 576 with 443 of them with all four reporter ions present. The CID-HCD approach identified a mean number of 282 proteins; 237 proteins were also quantified. On average, 1813 matching peptides were identified and 1728 peptides contained all iTRAQ channels. Even though PQD identified the smallest number of proteins, on average, 62 identified proteins (35%) were not quantified, whereas only 16% of the proteins identified with CID-HCD could not be quantified. Comparing the Mudpit Mascot protein scores achieved with the three methods, we obtained an average score of 62 for PQD, 99 for HCD and 148 for CID-HCD. As already mentioned, normalization of reporter ions resulted in an improvement of CID-HCD Mascot scores. Without normalization, we obtained an average Mascot protein score of 138, slightly lower than without normalization. In addition, the average number of identified proteins dropped from 281 proteins to 247 proteins. For all three methods, we obtained false discovery rates of less than 1% for the identified proteins, as determined by searching the data against a decoy database.

Accuracy of Quantitation with HCD, PQD and CID-HCD. Next, the data set was used to assess the standard deviations achievable with the three methods (Figure 5C). All three methods led to a geometric mean of the complete set of iTRAQ labeled peptides (channels 115/114) which was close to 1, the expected value, with similar standard deviations within each set of technical replicates. Interestingly, both HCD and CID-HCD had identical geometric standard deviations of approximately 1.2 (Figure 5), suggesting that the high collisional energy used in the CID-HCD approach did not distort the accuracy of HCD-based quantification. The standard deviation obtained with PQD was 2.0 (Figure 5), pointing to a much lower precision. Naturally, if a protein is identified and quantified with several peptides, the higher variance encountered with PQD might not be a problem. However, the geometric standard deviation achieved with PQD was still on average 1.47 for the complete set of identified proteins; therefore, quantification with PQD requires a significantly higher number of technical repeats.

Quantitative Characterization of an *in Vivo* Mouse Model of Cardiac Stress. Finally, we applied the CID-HCD method in a two-dimensional LC-MS/MS experiment. We used the technique to compare the protein expression in a mouse heart after transverse aortic constriction (TAC), an *in vivo* model of cardiac stress, to a control sample from an animal that received sham treatment.[38,39] This surgical procedure causes chronic pressure overload, resulting in a compensated concentric hypertrophy of the left ventricle within 2 weeks after intervention. The protein mixtures isolated from the left ventricles from both hearts were each digested with trypsin, split into two aliquots and labeled with iTRAQ. After mixing, peptides were separated by ion exchange chromatography. The fractions were analyzed by LC-MS/MS analysis using the CID-HCD method. The combined data set led to the identification of 1733 protein groups, based on 8321 unique peptides with a minimum Mascot ion score of 25 and a significance threshold of lower than 0.01 (Supplementary Table). Of the 8321 identified peptides, 7815 contained quantitative information from all iTRAQ reporter ions. With a value of 0.965, the mean ratio for iTRAQ 115/114 was close to 1 for these peptides, the expected value. The geometric standard deviation was 1.19, again corroborating the precision of the method. Within the identified 1733 protein groups, 1383 are quantified on the basis of at least two tandem mass spectra. Analyzing the iTRAQ ratios of the quantified proteins, we obtained a mean ratio of 0.96 for iTRAQ 115/114, 1.31 for iTRAQ 117/114 and 1.29 for iTRAQ 117/114 with geometrical standard deviations of 1.09. 1.21 and 1.23.

Next, the 1733 protein groups identified from the complete data set obtained in this analysis were analyzed with respect to their gene ontology (GO) annotation (Figure 6). According to their GO subcellular localization annotations, the majority of the identified proteins originate in the cytoplasm (1315), followed by localization to membranes (816). The most common molecular functions of the GO-annotated protein groups were found to be binding activities, such as and catalytic activity (1065), protein binding (959), metal ion binding (532), nucleotide binding (489) and transporter activity (251). GO-annotation to biological processes was most frequent for metabolic processes (1306), cell organization and biogenesis (555), regulation of biological processes (550) and transport (519). Analysis of the more than 1.5-fold up-regulated proteins by their GO annotation generated a similar picture. In the sample generated from the mouse heart which underwent transaortic constriction, we found 47 proteins up-regulated by a factor of 1.5 or more relative to the average iTRAQ ratios

(Table 1). We considered proteins which were 1.5-fold up-regulated in either channel, with the other channel within 10% of this value. This cutoff was well above the square of the standard deviation which was 1.4 for both channels. We only found 15 proteins down-regulated by a factor of 0.67 or more in our sample. We conclude that down-regulation is less pronounced than up-regulation in our *in vivo* model of cardiac stress. The same criterion was applied for the down-regulated proteins (Table 2).

When some prominent species of the proteins up-regulated more than 1.5-fold in the TAC model are analyzed in detail, the most pronounced hits, ANKRD1 is preferentially expressed in hearts and was previously shown to be up-regulated in response to stress and hypertrophic stimuli and in heart failure.[40] Periostin was also reported to be linked to cardiac hypertrophy due to myocardial infarction and was shown to induce proliferation of differentiated cardiomyocytes.[41] FHL1 was suggested to play an important role in biomechanical stress responses involved in cardiac hypertrophy and disease. Fhl1 was shown to be up-regulated in mouse hearts subsequent to *in vivo* pressure overload induced hypertrophy and hypertrophic agonists and FHL1 was reported to be up-regulated after TAC but not the other members of its respective protein family.[42] Further, it was shown that overexpression of HSPB6, the cardiac HSP20 in cardiomyocytes significantly increased intracellular Ca^{2+} transient and contraction amplitudes, indicating that HSP20 is involved in the regulation of myocardial contractility.[43] SERPIN1, the pro-collagen-specific chaperone protein, was also found to be up-regulated, similarly to the most abundant small heat shock protein CRYAB, which is also known for its cardio-protective role. Translationally controlled tumor protein (TPT1) was published to repress Na^+,K^+-ATPase activity and thereby indirectly increase myocardial contractility.[44]

Conclusions

We have shown that the CID-HCD approach is capable of outperforming PQD and HCD for peptide quantification and identification. The superiority of the novel method was most pronounced in the number of identified peptides in LC-MS/MS experiments analyzing complex peptide mixtures where the CID-HCD approach identified and quantified approximately 3 times more peptides than PQD, resulting in a more than 2 times higher number of quantified proteins. In addition, the technique proved to be better suited for analysis of minute amounts of proteins than HCD alone. The higher ion counts achievable with HCD and the combined approach resulted in a vast improvement of the accuracy of protein quantitation. We have furthermore demonstrated the practical utility of the method by determining protein expression changes in an *in vivo* mouse model of cardiac hypertrophy.

Acknowledgment. This work was funded by the Austrian Proteomics Platform (APP) within the Austrian Genome Research Program (GEN-AU) and the Institute of Molecular Pathology (IMP). We thank the other members of the Mechtler group, especially Ines Steinmacher and Michael Mazanek for experimental help and Goran Mitulovic, Johann Holzmann and James Hutchins for critical reading of the manuscript.

Supporting Information Available: Supplementary Table, protein groups identified and quantified are listed with their corresponding iTRAQ ratios, Mascot (MudPIT) protein scores and the identifying peptides. This material is available free of charge via the Internet at http://pubs.acs.org.

References

(1) Domon, B.; Aebersold, R. *Science* **2006**, *312*, 212–217.
(2) Aebersold, R.; Mann, M. *Nature* **2003**, *422*, 198–207.
(3) Han, X. M.; Aslanian, A.; Yates, J. R. *Curr. Opin. Chem. Biol.* **2008**, *12*, 483–490.
(4) Kocher, T.; Superti-Furga, G. *Nat. Methods* **2007**, *4*, 807–815.
(5) Jensen, O. N. *Curr. Opin. Chem. Biol.* **2004**, *8*, 33–41.
(6) Ong, S. E.; Mann, M. *Nat. Chem. Biol.* **2005**, *1*, 252–262.
(7) Bantscheff, M.; Schirle, M.; Sweetman, G.; Rick, J.; Kuster, B. *Anal. Bioanal. Chem.* **2007**, *389*, 1017–1031.
(8) Hood, L.; Heath, J. R.; Phelps, M. E.; Lin, B. Y. *Science* **2004**, *306*, 640–643.
(9) Tackett, A. J.; DeGrasse, J. A.; Sekedat, M. D.; Oeffinger, M.; Rout, M. P.; Chait, B. T. *J. Proteome Res.* **2005**, *4*, 1752–1756.
(10) Gerber, S. A.; Rush, J.; Stemman, O.; Kirschner, M. W.; Gygi, S. P. *Proc. Natl. Acad. Sci. U.S.A.* **2003**, *100*, 6940–6945.
(11) Hochleitner, E. O.; Kastner, B.; Frohlich, T.; Schmidt, A.; Luhrmann, R.; Arnold, G.; Lottspeich, F. *J. Biol. Chem.* **2005**, *280*, 2536–2542.
(12) Wepf, A.; Glatter, T.; Schmidt, A.; Aebersold, R.; Gstaiger, M. *Nat. Methods* **2009**, *6*, 203–205.
(13) Kruger, M.; Kratchmarova, I.; Blagoev, B.; Tseng, Y. H.; Kahn, C. R.; Mann, M. *Proc. Natl. Acad. Sci. U.S.A.* **2008**, *105*, 2451–2456.
(14) Yi, E. C.; Li, X. J.; Cooke, K.; Lee, H.; Raught, B.; Page, A.; Aneliunas, V.; Hieter, P.; Goodlett, D. R.; Aebersold, R. *Proteomics* **2005**, *5*, 380–387.
(15) Mann, M. *Nat. Rev. Mol. Cell Biol.* **2006**, *7*, 952–958.
(16) Gygi, S. P.; Rist, B.; Gerber, S. A.; Turecek, F.; Gelb, M. H.; Aebersold, R. *Nat. Biotechnol.* **1999**, *17*, 994–999.
(17) Ross, P. L.; Huang, Y. L. N.; Marchese, J. N.; Williamson, B.; Parker, K.; Hattan, S.; Khainovski, N.; Pillai, S.; Dey, S.; Daniels, S.; Purkayastha, S.; Juhasz, P.; Martin, S.; Bartlet-Jones, M.; He, F.; Jacobson, A.; Pappin, D. J. *Mol. Cell. Proteomics* **2004**, *3*, 1154–1169.
(18) Rappsilber, J.; Mann, M. *Trends Biochem. Sci.* **2002**, *27*, 74–78.
(19) Nesvizhskii, A. I.; Aebersold, R. *Mol. Cell. Proteomics* **2005**, *4*, 1419–1440.
(20) Choe, L.; D'Ascenzo, M.; Relkin, N. R.; Pappin, D.; Ross, P.; Williamson, B.; Guertin, S.; Pribil, P.; Lee, K. H. *Proteomics* **2007**, *7*, 3651–3660.
(21) Han, H. L.; Pappin, D. J.; Ross, P. L.; McLuckey, S. A. *J. Proteome Res.* **2008**, *7*, 3643–3648.
(22) Phanstiel, D.; Zhang, Y.; Marto, J. A.; Coon, J. J. *J. Am. Soc. Mass Spectrom.* **2008**, *19*, 1255–1262.
(23) DeSouza, L.; Diehl, G.; Rodrigues, M. J.; Guo, J. Z.; Romaschin, A. D.; Colgan, T. J.; Siu, K. W. M. *J. Proteome Res.* **2005**, *4*, 377–386.
(24) Hardt, M.; Witkowska, H. E.; Webb, S.; Thomas, L. R.; Dixon, S. E.; Hall, S. C.; Fisher, S. J. *Anal. Chem.* **2005**, *77*, 4947–4954.
(25) Hardman, M.; Makarov, A. A. *Anal. Chem.* **2003**, *75*, 1699–1705.
(26) Hu, Q. Z.; Noll, R. J.; Li, H. Y.; Makarov, A.; Hardman, M.; Cooks, R. G. *J. Mass Spectrom.* **2005**, *40*, 430–443.
(27) Perry, R. H.; Cooks, R. G.; Noll, R. J. *Mass Spectrom. Rev.* **2008**, *27*, 661–699.
(28) Griffin, T. J.; Xie, H. W.; Bandhakavi, S.; Popko, J.; Mohan, A.; Carlis, J. V.; Higgins, L. *J. Proteome Res.* **2007**, *6*, 4200–4209.
(29) Olsen, J. V.; Macek, B.; Lange, O.; Makarov, A.; Horning, S.; Mann, M. *Nat. Methods* **2007**, *4*, 709–712.
(30) Jacobshagen, C.; Gruber, M.; Teucher, N.; Schmidt, A. G.; Unsold, B. W.; Toischer, K.; Van, P. N.; Maier, L. S.; Kogler, H.; Hasenfuss, G. *Eur. J. Heart Failure* **2008**, *10*, 334–342.
(31) Olsen, J. V.; de Godoy, L. M. F.; Li, G. Q.; Macek, B.; Mortensen, P.; Pesch, R.; Makarov, A.; Lange, O.; Horning, S.; Mann, M. *Mol. Cell. Proteomics* **2005**, *4*, 2010–2021.
(32) Meany, D. L.; Xie, H. W.; Thompson, L. V.; Arriaga, E. A.; Griffin, T. J. *Proteomics* **2007**, *7*, 1150–1163.
(33) Bantscheff, M.; Boesche, M.; Eberhard, D.; Matthieson, T.; Sweetman, G.; Kuster, B. *Mol. Cell. Proteomics* **2008**, *7*, 1702–1713.
(34) Zubarev, R.; Mann, M. *Mol. Cell. Proteomics* **2007**, *6*, 377–381.
(35) Liu, T.; Belov, M. E.; Jaitly, N.; Qian, W. J.; Smith, R. D. *Chem. Rev.* **2007**, *107*, 3621–3653.
(36) Guo, T.; Gan, C. S.; Zhang, H.; Zhu, Y.; Kon, O. L.; Sze, S. K. *J. Proteome Res.* **2008**, *7*, 4831–4840.
(37) Lopez, L. L.; Tiller, P. R.; Senko, M. W.; Schwartz, J. C. *Rapid Commun. Mass Spectrom.* **1999**, *13*, 663–668.
(38) Rockman, H. A.; Ross, R. S.; Harris, A. N.; Knowlton, K. U.; Steinhelper, M. E.; Field, L. J.; Ross, J.; Chein, K. R. *Proc. Natl. Acad. Sci. U.S.A.* **1991**, *88*, 8277–8281.

(39) Hu, P.; Zhang, D. F.; Swenson, L.; Chakrabarti, G.; Abel, E. D.; Litwin, S. E. *Am. J. Physiol.: Heart Circ. Physiol.* **2003**, *285*, H1261–H1269.
(40) Mikhailov, A. T.; Torrado, M. *Int. J. Dev. Biol.* **2008**, *52*, 811–821.
(41) Kuhn, B.; del Monte, F.; Hajjar, R. J.; Chang, Y. S.; Lebeche, D.; Arab, S.; Keating, M. T. *Nat. Med.* **2007**, *13*, 962–969.
(42) Chu, P. H.; Ruiz-Lozano, P.; Zhou, Q.; Cai, C. L.; Chen, J. *Mech. Dev.* **2000**, *95*, 259–265.
(43) Chu, G. X.; Egnaczyk, G. F.; Zhao, W.; Jo, S. H.; Fan, G. C.; Maggio, J. E.; Xiao, R. P.; Kranias, E. G. *Circ. Res.* **2004**, *94*, 184–193.
(44) Kim, M. J.; Kwon, J. S.; Suh, S. H.; Suh, J. K.; Jung, J. H.; Lee, S. N.; Kim, Y. H.; Cho, M. C.; Oh, G. T.; Lee, K. L. *J. Mol. Cell. Cardiol.* **2008**, *44*, 151–159.

PR900451U